# Numerical and parametric analyses of four unreinforced embankments on soft soils

Naloan C. Sampa[1], Laura Z. Sassi[1]

[1]*Dept. of Civil Engineering, Federal University of Santa Catarina*
*João Pio Duarte da Silva - 205, 88040-900, Santa Catarina, Brazil*
*naloan.sampa@ufsc.br, lazasassi@gmail.com*

**Abstract.** This study conducts forty numerical simulations to evaluate the performance of four unreinforced embankments on soft soils, considering a variety of geometries and soil properties. The embankments, composed of granular materials, exhibit dimensions of 3.5 m in height and 17 m in width. The underlying soft soil layer extends horizontally for 30 m, with thicknesses varying from 5 m to 20 m. Geotechnical parameters representative of the Florianópolis/Brazil are employed. The behaviour of the soft soil is characterized using the Modified Cam Clay model, while the response of the embankment material is modelled using the Mohr-Coulomb model. The investigation assesses the influence of slope of the critical state line ($M$), recompression index ($\kappa$), overconsolidation ratio ($0CR$) and thickness of soft soil ($H_s$) on critical factors such as the distribution of effective vertical stress, settlement patterns, excess pore water pressure distribution, lateral displacement profiles, and deformation rate. The paper identifies key parameters governing embankment performance and discusses their implications for embankment stability and deformation.

**Keywords:** settlement, excess pore pressure, distortion, displacement, Abaqus.

## 1 Introduction

A comprehensive investigation into embankments behavior is necessary due to the expansion of urban areas, demand for improved services and communications, development of industry, land reclamation in overpopulated areas, and the development of infrastructure on soft soils. Construction and design techniques, as well as monitoring methods, are utilized to ensure the stability, calculate the rate and magnitude of deformation, and analyze the performance of embankments during and after construction. The stability, deformability, and performance aspects of structures have been extensively examined in numerous studies (Ryde [1], Almeida and Marques [2], Massad [3]).

Settlement, lateral displacement, and pore pressure analysis are emphasized to prevent structural collapse (Ryde [1], Brugger [4]). Traditionally, One-Dimensional Consolidation Theory (Terzaghi [5], Terzaghi and Fröhlich [6]) has been used for settlement estimation, and limit equilibrium methods (Fellenius [7], Bishop [8], Morgenstern and Price [9], and others) have been used for stability analysis. Finite Element Methods have enabled sophisticated numerical modelling for analyzing stability and deformability in complex scenarios (Ryde [1]).

This study aims to evaluate the performance of 4 typical unreinforced embankments on soft soils by analyzing settlement, horizontal displacement, pore pressure, and increase in effective stress concerning various geotechnical and geometrical parameters. The traditional method of analyzing stability by calculating the safety factor is beyond the scope of this paper.

## 2 Numerical and parametric analysis

Four 2D numerical models were created using Abaqus finite element software to simulate granular material embankments over soft clay layers of varying thicknesses. The embankments had a height ($H_e$) of 3.5 m, a width of 20 m at the crest, and slopes at a 1:2 ratio (vertical to horizontal). The foundation, represented by soft clay, was 60 m in length. To account for symmetry, the model only includes half of the embankment-foundation domain and assumes a plane strain condition. Figure 1 depicts half of the model domain, with the letter '$H_S$' denoting the thickness of the soft clay layer (5 m, 10 m, 15 m and 20 m).

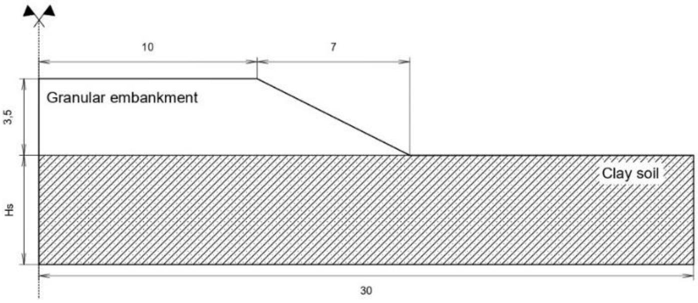


Figure 1. Half-domain of the numerical model, in m.

The embankment was modeled as a homogeneous, dry solid body using the Mohr-Coulomb plasticity criterion. The soft clay foundation was simulated under saturated conditions with elastoplastic behavior, employing the Modified Cam Clay model. The typical parameters of soft soils from Florianópolis-Brazil and grain materials were utilized, as shown in Tables 1 and 2, respectively. For additional information on soft soils in Florianópolis, readers are encouraged to refer to Oliveira [10].

Table 1. Parameters of the clay soil.

| Parameter | Value |
|---|---|
| Initial void ratio - $e_0$ | 2.5 |
| Bulk unit weight - $\gamma$ (kN/m³) | 15 |
| Recompression index - $\kappa$ | 0.065 |
| Poisson's ratio - $\nu$ | 0.33 |
| Compression index - $\lambda$ | 0.65 |
| Slope of the critical state line - $M$ | 1 |
| Initial size of the yield surface - $p'/\sigma'_{v0}$ | 0.75, 1.0, 1.5 and 3.0 |
| Size of the yield surface in the wet side - $\beta$ | 1 |
| Ratio of the flow stress - $K$ | 1 |
| Permeability coefficient - $k$ (m/s) | 2.50E-08 |
| Lateral earth pressure at rest – $K_0 = 1 - \text{sen}\,\phi$ | 0.57 |

Table 2. Parameters of the embankment material

| Parameter | Value |
|---|---|
| Initial void ratio - $e_0$ | 0.65 |
| Bulk unit weight - $\gamma$ (kN/m³) | 20 |
| Cohesion - $c$ (kN/m²) | 2 |
| Internal friccional angle - $\phi$ (º) | 30 |
| Dilatancy - $\psi$ (º) | 0 |
| Elastic Module - $E$ (kN/m²) | 1000 |
| Poisson's ratio - $\nu$ | 0.3 |
| Permeability coefficient - $k$ (m/s) | 0.01 |

The numerical simulations were conducted in three stages. Firstly, initial geostatic stresses were established in the foundation layer. Secondly, the embankment was progressively constructed over one month. Finally, the embankment's behavior (settlement, horizontal displacement, pore pressure, and effective stress) was monitored during 48 months (4 years) consolidation process.

To replicate real embankment conditions on soft soils under plane strain condition, physical and drainage boundary conditions were established. The base of the model had fixed vertical (U2=0) and horizontal (U1= 0) displacements, while only horizontal displacement (U1=0) was restricted on the sides. The foundation layer surface was permeable, maintaining zero pore pressure (U8= 0). The drainage boundary conditions at the soil surface were constant throughout all simulation stages. Figure 2 demonstrates the implemented boundary conditions.

Figure 3 shows the mesh discretization of a numerical model with a 5 m soft soil layer. The same approach was used for soil thicknesses of 10 m, 15 m, and 20 m. Mesh refinement was applied in areas of high stress and deformation, with element sizes increasing away from the embankment base and soil surface.

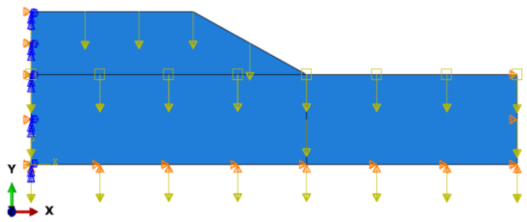


Figure 2. Boundary conditions.

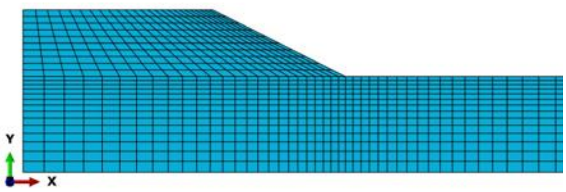


Figure 3. Mesh discretization of the model.

Two types of 2D solid quadrilateral finite elements were used: CPE8RP for the soil foundation and CPE8R for the embankment. The embankment domain consisted of 250 elements, while the soil domain, with thicknesses ranging from 5 m to 20 m, was modelled with 630 to 1125 elements.

Forty parametric analyses were conducted across four numerical models to investigate the impact of soil thickness ($H_s$), slope of critical state line ($M$), recompression index ($\kappa$), and overconsolidation ratio ($OCR$) on excess pore pressure ($\Delta u$), vertical effective stress ($\sigma'_v$), settlement ($\rho$), horizontal displacement ($\delta_h$), and distortion.

Each model underwent 10 analyses, with analysis 1 as the reference. In subsequent analyses, one parameter was modified within the established ranges while others remained constant with reference values. Table 3 outlines the varied parameters and their corresponding values for each of the 10 analyses. The $OCR$ of 0.75 does not have a physical meaning; it was used solely for investigative purposes.

Results from 11 designated points, 3 horizontal lines, and 6 vertical lines shown in Fig. 4 were exported from Abaqus to Excel. The point data is intended for time-dependent analyses, while the data from vertical lines facilitate depth-wise analyses. The data from horizontal lines are analysed across the width of the soil or embankment, taking into account periods of 1 month (at the end of embankment construction) and 48 months.

Table 3. Parametric analysis.

| Analysis | M | κ | OCR |
|---|---|---|---|
| Analysis 1 (reference) | 1 | 0.065 | 1.00 |
| Analysis 2 | 1.1 | - | - |
| Analysis 3 | 1.2 | - | - |
| Analysis 4 | 1.3 | - | - |
| Analysis 5 | - | 0.05 | - |
| Analysis 6 | - | 0.08 | - |
| Analysis 7 | - | 0.095 | - |
| Analysis 8 | - | - | 0.75 |
| Analysis 9 | - | - | 1.50 |
| Analysis 10 | - | - | 3.00 |

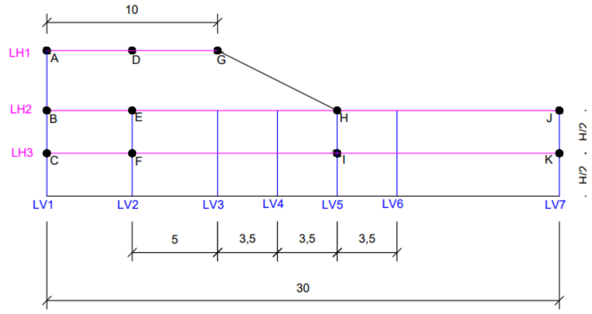


Figure 4. Points and lines used for data extraction.

## 3 Numerical and parametric analysis

Due to the limitations of number of pages, this section presents only the principal results of the study.

### 3.1 Settlement (vertical displacement)

The objective of settlement analysis is to comprehend embankment performance and qualitatively assess stability. Settlements were analyzed at 11 points over time and along horizontal lines at 1 month and 48 months.

Two normalization methods are shown in Fig. 5 to illustrate the effect of the parameter $M$ on settlement of the soft soil. The curves of this figure indicate the most significant settlements in the central region of the embankment. Soil settlement under the embankment causes horizontal displacement and uplift of the soil near the slope's toe, which decreases significantly over time after embankment construction.

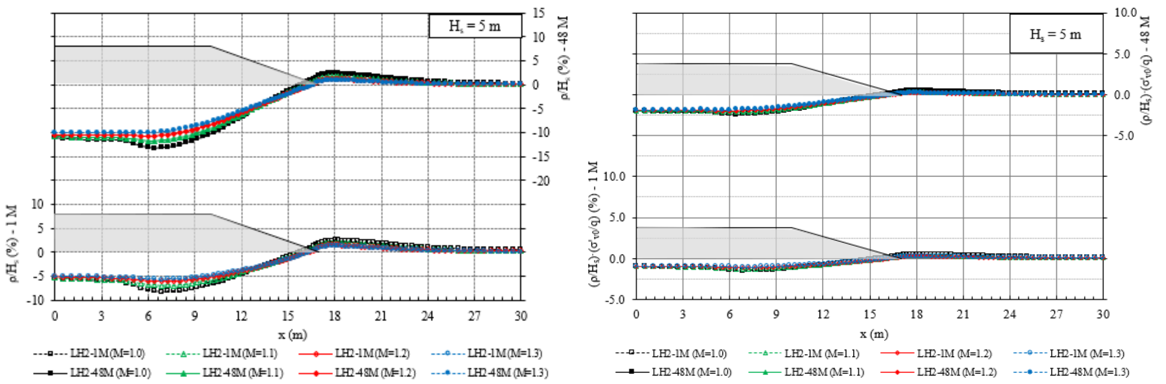

Figure 5. Normalized settlements along the line LH2.

Increasing the thickness of soft clay ($H_s$) generally decreases the normalized settlement ($\rho/H_s$) under consistent soil characteristics. The impact of variations in parameters $M$ and $OCR$ on $\rho/H_s$ is negligible, particularly for $H_s \geq 10$ m (Fig. 6).

Regardless of $H_s$ value, increasing parameter $\kappa$ reduces $\rho/H_s$. The maximum $\rho/H_s$ tends to occur not at the symmetry axis, but slightly before the embankment slope for $H_s \geq 10$ m. At the symmetry axis, $\rho/H_s$ varies between 1.91% and 3.56% for $H_s$ of 20 m, between 2.25% and 4.22% for $H_s$ of 15 m, between 4.39% and 7.99% for $H_s$ of 10 m, and between 4.22% and 15.00% for $H_s$ of 5 m.

Settlement results, normalized as $(\rho/H_s)\cdot(\sigma'_{v0}/q)$ in Fig. 5, are minimally affected by $H_s$. The increase in $\kappa$ slightly reduces $(\rho/H_s)\cdot(\sigma'_{v0}/q)$ for $H_s \geq 10$ m. The impact of $M$ and $OCR$ in $(\rho/H_s)\cdot(\sigma'_{v0}/q)$ is observed only in analyses with $H_s = 5$ m.

Figure 7 illustrates the correlation between $\rho/H_s$ and square root of time ($\sqrt{t}$) for points A and H. Point H at the toe of slope exhibits significant upward displacement, which increased during embankment construction and decreased afterward. Further investigation is required to explain this reversal of displacement.

An increase in $H_s$ does not significantly affect the settlement stabilization time ($T_{set}$). For $H_s \geq 10$ m, $T_{set}$ tends to stabilize with $M > 1$, $\kappa > 0.065$, and $OCR > 1$. Analyses with $H_s = 5$ m show that variations in $M$ and $\kappa$ have no significant influence on $T_{set}$. However, $T_{set}$ decreases as $OCR$ values increase from 0.75 to 3. The time interval between the end of embankment construction and $T_{set}$ ranges from 5.2 to 12.9 months.

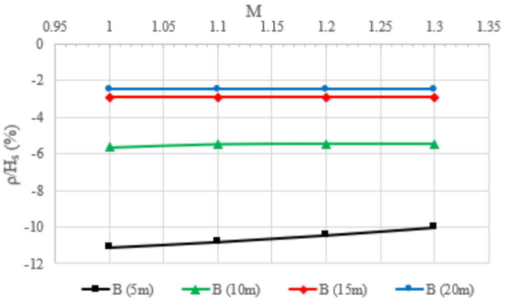


Figure 6. The influence of the $M$ on the $\rho/H_s$.

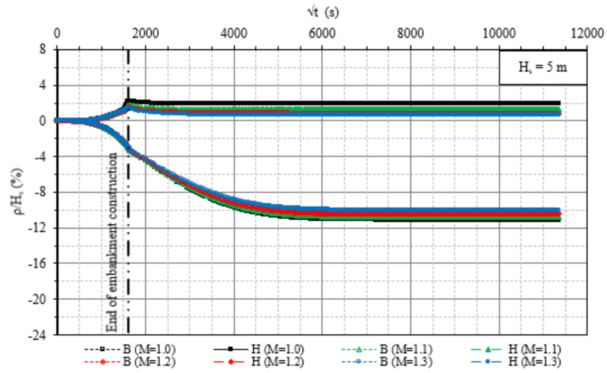


Figure 7. Variation of $\rho/H_s$ versus $\sqrt{t}$.

### 3.2 Horizontal displacement

Assessing embankment stability requires a thorough investigation of the horizontal displacement evolution over time. Significant horizontal displacements may result in the development of shear stress and embankment failure.

Figure 8 demonstrates the variation of normalized horizontal displacement ($\delta_h/H_e$) along the depth of the LV5 for analysis with $H_s$ of 5 m and 10 m. The $(\delta_h/H_e)_{max}$ usually occurs at the surface of the soft soil, except for LV3 and certain analyses with $H_s = 5$ m. Parameter variations in $M$ and $OCR$ only affect $\delta_h/H_e$ for $H_s = 5$ m. When varying the $M$ along LV5, $(\delta_h/H_e)_{max}$ ranges from 5.5% to 9.5% for $H_s = 5$ m, and from 8.7% to 4.4% for $H_s = 10$ m, 15 m, and 20 m. Similarly, when varying the $OCR$ along LV5, $(\delta_h/H_e)_{max}$ ranges from 4.6% to 21.0% for $H_s = 5$ m, and from 8.4% to 4.2% for $H_s = 10$ m, 15 m, and 20 m. The variation of the $\kappa$ influences $\delta_h/H_e$ for all $H_s$ values, with increasing $\kappa$ leading to increased $\delta_h$. Along LV5, $(\delta_h/H_e)_{max}$ varies from 7.7% to 12.5%, 6.5% to 12.7%, 3.7% to 7.3%, and 3.1% to 6.3% for $H_s = 5$ m, 10 m, 15 m, and 20 m, respectively.

In most cases, $(\delta_h/H_e)_{max}$ is below 10%. However, there was a critical situation where $(\delta_h/H_e)_{max}$ reached 21% in the analyses with $OCR = 0.75$ and $H_s = 5$ m.

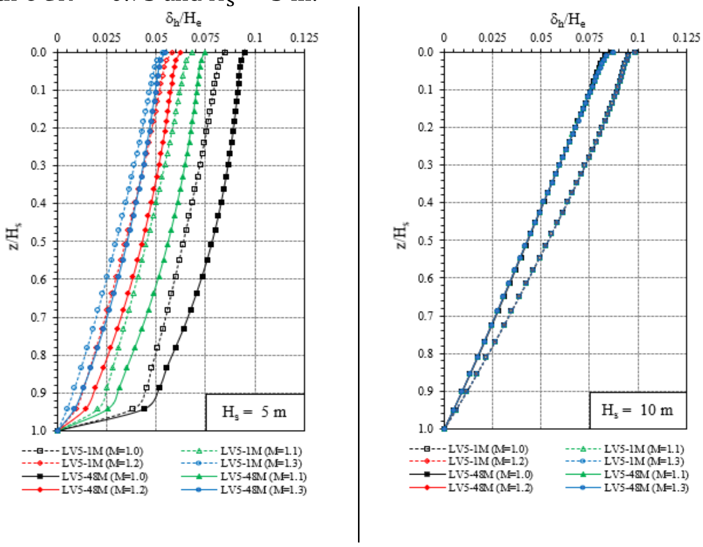


Figure 8. Variation of $\delta_h/H_e$ along the normalized depth.

The configuration of $\delta_h/H_e$ curves of LV3 typically demonstrates a curvilinear trend along the normalized depth $z/H_s$. In these cases, $\delta_h/H_e$ tends to show small variation between the clay surface and $z/H_s$, which ranges from 0.6 to 0.8. Analyses with $H_s \geq 10$ m show linear configurations of $\delta_h/H_e$ curves for LV5 and LV6, indicating a nearly linear decrease in $\delta_h/H_e$ values with an increase in $z/H_s$. Conversely, analyses with $H_s = 5$ m exhibit a curvilinear pattern for $\delta_h/H_e$ along all vertical lines (LV3, LV5 and LV6).

The horizontal displacements along the depth at 1 month exceed final horizontal displacements, except for analyses with $H_s = 5$ m. This reversal is likely due to soil consolidation mechanisms or numerical model characteristics, with its intensity increasing with $H_s$. Variations in $M$ and $\kappa$ minimally impact the magnitude of this reversal for $H_s \geq 10$ m. Variation of $OCR$ has a greater impact than $M$, which in turn exceeds the influence of variation of $\kappa$ on the reversal of horizontal displacement.

As expected, in Fig. 9, the horizontal displacement and the horizontal volume ($V_h$) of the soft soil decrease with the distance from the slope. Specifically, the $V_h$ values of line LV3 are higher than those of line LV5, which are higher than those of line LV6. In all analyses, the horizontal displacement values are greater than zero around the maximum soil depth ($z/H_s = 1$), indicating soil mobilization to deeper depths. This highlights the insufficiency of all soft soil thicknesses in limiting horizontal displacement at the base of the numerical models.

For $H_s \geq 10$ m, both horizontal volume ($V_h$) and vertical volume below the embankment ($V_{v1}$) decrease slightly with increasing $H_s$ and remain relatively stable with variations in $M$, $\kappa$, and $OCR$ (see Fig. 9). Conversely, for analyses with $H_s = 5$ m, $V_h$ and $V_{v1}$ tend to decrease with increasing $M$ and $OCR$, while increasing with increasing $\kappa$.

The intensity of soil displacement reversal is assessed by the ratio $V_{v1}/V_{v2}$, representing the vertical soil volumes mobilized below the embankment ($V_{v1}$) to those mobilized upward around the toe ($V_{v2}$). At 48 months (and 1 month), $V_{v1}/V_{v2}$ varies between 4.66 and 23.42 (3.02 and 10.28) for $H_s = 5$m, 14.05 and 16.24 (4.36 and 5.17) for $H_s = 10$ m, 17.85 and 18.05 (4.59 and 5.35) for $H_s = 15$ m, and 22.47 and 22.61 (4.50 and 5.11) for $H_s = 20$ m.

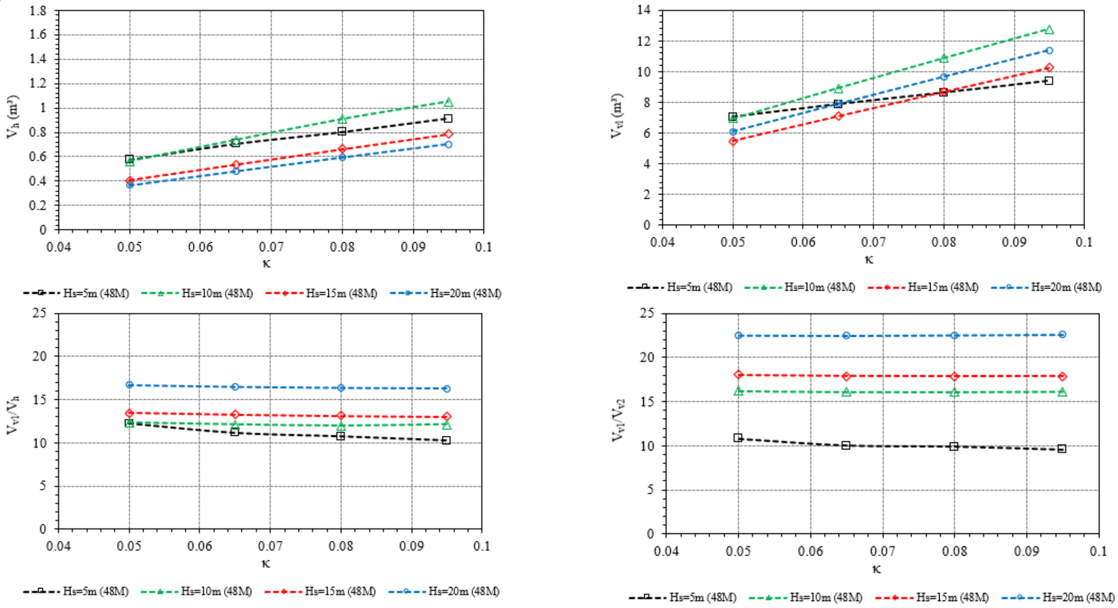

Figure 9. Horizontal and vertical volume of soils.

Figure 10 demonstrates the variation of the total distortion, calculated as $\mathrm{atan}\{(\delta_{h2} - \delta_{h1})/(z_2 - z_1)\}$, along the normalized depth. The parameters $M$ and $OCR$ affect the percentage of total distortion in analyses with $H_s = 5$ m. Regardless of the $H_s$ value, an increase in $\kappa$ results in increased total distortion in lines LV3, LV5, and LV6, with the total distortion varying along depth depending on line position.

In analyses with $H_s = 5$ m, total distortion tends to increase slightly with normalized depth. With the exception of analyses where $OCR = 0.75$, most analyses with $H_s = 5$ m have a maximum total distortion of less than 10% at $z/H_s$ below 0.85. Conversely, for analyses with $H_s \geq 10$ m, the total distortion stabilizes at greater depths and typically remains below 2%, especially for analyses with $H_s$ of 15 m and 20 m.

The total distortion decreases as the soft soil thickness increases, particularly when $H_s \geq 10$ m. For normalized depths less than 0.45, the deformations in analyses with $H_s = 5$ m are less than those in analyses with $H_s = 10$ m. In all analyses, the deformation rate remains well below 0.5% per day, indicating slope stability as reported by Almeida and Marques [2].

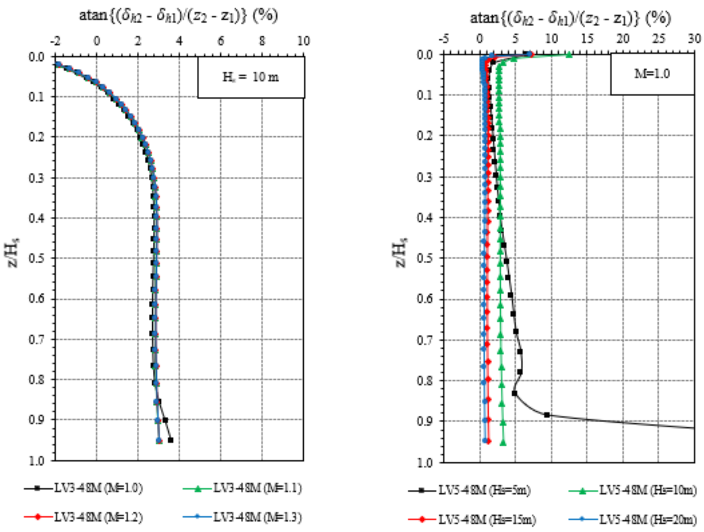

Figure 10. Total distortion versus the normalized depth.

### 3.3 Excess pore water pressure

Assessing consolidation evolution and resulting increases in effective stress and factor of safety in soft soil requires evaluating excess pore pressure.

The following results (Fig. 11) concern the completion of embankment construction over a one-month period. The analyses indicate that excess pore pressure ($\Delta u$) increases with depth and proximity to the centerline of the numerical model.

The normalized excess pore pressure ($\Delta u/q$) (Fig. 11) is not affected by the variation of parameters $M$ and $OCR$ when $H_s \geq 10$ m. q represents the stress of 70 kPa applied by the embankment on the soft soil surface. In analyses with varying parameter $\kappa$ and for $H_s = 5$ m, an opposite trend is noted regardless of the position of the vertical lines. Increasing $\kappa$ leads to an increase in excess pore pressure. Figure 14 illustrates the variation of $\Delta u/q$ with normalized depth ($z/H_s$).

The curves of $\Delta u/q$ versus $z/H_s$ for lines LV1 to LV5 generally exhibit similar behavior, showing a linear growth of $\Delta u/q$ at shallower depths and constancy at greater depths. In contrast, the curves for line LV2 exhibit an opposite behavior. Specifically, for a given depth, $\Delta u/q$ tends to increase with the thickness of the soft soil $H_s$. However, contrary to expectations, it was observed that, particularly at greater depths, the $\Delta u/q$ for analyses with $H_s = 10$ m are higher than those for analyses with $H_s = 15$ m.

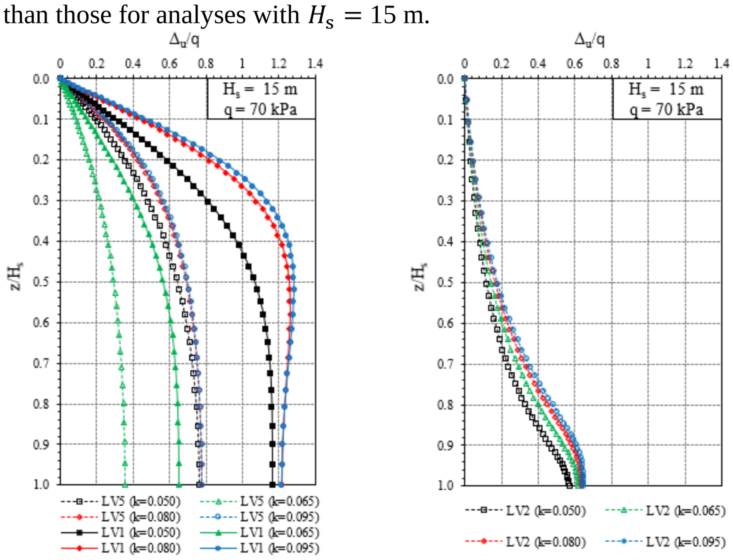

Figure 11. Variation of $\Delta u/q$ along the normalized depth.

## 4 Conclusions

This paper presents the results of 40 numerical simulations investigating the effects of $M, OCR, \kappa,$ and $H_s$ on excess pore pressure, settlement, horizontal displacement, distortion, and soil mobilization in landfills on soft soils. The key conclusions are important for future stability and deformability analyses.

Increasing $H_s$ generally decreases $\rho/H_s$. For analyses with $H_s \geq 10$ m, the increase in κ slightly reduces $\rho/H_s$ and the impact of variations in parameters $M$ and $OCR$ on $\rho/H_s$ is negligible. The maximum $\rho/H_s$ tends to occur slightly before the embankment slope, rather than at the symmetry axis. At the symmetry axis, $\rho/H_s$ varies between 1.91% and 15.0%;

Point H, at the toe of slope, exhibits significant upward displacement, which increased during embankment construction and decreased afterward. The reversal behavior is also observed with $\delta_h$ and $V_h$. This reversal is likely due to soil consolidation mechanisms or numerical model characteristics, with its intensity increasing with $H_s$. $OCR$ has a greater impact than $M$, which in turn exceeds the influence of $\kappa$ on the reversal of $\delta_h$;

An increase in $H_s$ does not significantly affect the $T_{set}$. For $H_s \geq 10$ m, $T_{set}$ tends to stabilize with $M > 1$, $\kappa > 0.065$, and $OCR > 1$. The time interval between the end of embankment construction and $T_{set}$ ranges from 5.2 to 12.9 months;

The $(\delta_h/H_e)_{max}$ usually occurs at the surface of the soft soil, except for Line LV3 and certain analyses with $H_s = 5$ m. $M$ and $OCR$ only affect $\delta_h/H_e$ for $H_s = 5$ m, while $\kappa$ influences $\delta_h/H_e$ for all $H_s$ values, with increasing $\kappa$ leading to increased $\delta_h/H_e$. In most cases, $(\delta_h/H_e)_{max}$ is below 10%;

For $H_s \geq 10$ m, both $V_h$ and $V_{v1}$ decrease slightly with increasing $H_s$ and remain relatively stable with variations in $M$, $\kappa$, and $OCR$. Conversely, for analyses with $H_s = 5$ m, $V_h$ and $V_{v1}$ tend to decrease with increasing $M$ and $OCR$, while increasing with increasing $\kappa$;

$M$ and $OCR$ affect total distortion in analyses with $H_s = 5$ m. Regardless of the $H_s$ value, an increase in $\kappa$ results in increased total distortion. In analyses with $H_s = 5$ m, total distortion tends to increase slightly with normalized depth. For analyses with $H_s \geq 10$ m, the total distortion stabilizes at greater depths and typically remains below 2%, especially for analyses with $H_s = 15$ m and 20 m. The total distortion decreases as the soft soil thickness increases, particularly when $H_s \geq 10$ m. In all analyses, the distortion rate remains well below 0.5% per day, indicating slope stability as reported by Almeida and Marques [2];

The excess pore pressure ($\Delta u$) increases with depth and proximity to the centerline of the numerical model. The normalized excess pore pressure ($\Delta u/q$) is not affected by $M$ and $OCR$ when $H_s \geq 10$ m. In analyses with varying parameter $\kappa$ and for $H_s = 5$ m, an opposite trend is noted regardless of the position of the vertical lines. Increasing $\kappa$ leads to an increase in excess pore pressure;

The quality of the analysis results underscores the effectiveness of Abaqus software in assessing the performance of geotechnical structures that require monitoring of excess pore press.

**Authorship statement.** The authors hereby confirm that they are the sole liable persons responsible for the authorship of this work, and that all material that has been herein included as part of the present paper is either the property (and authorship) of the authors, or has the permission of the owners to be included here.

## References

[1] S.J, Ryde. The performance and backanalysis of embankments on soft estuarine clay. Doctor of Philosophy, Department of Civil Engineering, University of Bristol, 1977.
[2] M. S. S, Almeida, M. E. S, Marques. Aterros sobre solos moles: projeto e desempenho (Embankments on Soft Soils: Design and Performance). São Paulo: Oficina de Textos, 2010. [in Portuguese]
[3] F. Massad. Obras de Terra: curso básico de geotecnia (Earthworks: Basic Course in Geotechnics). 2. ed. São Paulo: Oficina de Textos, 2010. [in Portuguese]
[4] P.J. Brugger. Análise de deformações em aterros sobre solos moles (Deformation analysis of embankments on soft soils. Doctor of Philosophy, Department of Science of Civil Engineering, Federal University of Rio de Janeiro, 1996. [in Portuguese]
[5] K. Terzaghi. Erdbaumechanick, Viena, Franz Deutcke, Áustria, 1925. [In German]
[6] K. Terzaghi, O. K. Frölich. Thoerie der setzung von tonschichten. Franz Deuticke, Leipzig, 1936. [In Germann
[7] W. Fellenius. Calculation of the Stability of Earth Dams. Transactions. 2nd Congress Large Dams. Vol. 4 (445), 1936.
[8] A. W. Bishop. The use of the slip circle in the stability analysis of slopes. Géotechnique. Vol. 5 (1), pp. 7-17, 1955.
[9] N.R. Morgenstern. Price, V.E. The analysis of the stability of general slip surfaces. Géotechnique. Vol. 15 (1), pp. 79-93, 1965.
[10] H.M. Oliveira. Comportamento de aterros reforçados sobre solos moles levados a ruptura (Behavior of reinforced embankments on soft soils led to rupture). Doctor of Philosophy, Department of Science of Civil Engineering, Federal University of Rio de Janeiro, 2006. [in Portuguese].